

Design and synthesis of thiobarbituric acid analogues as potent urease inhibitors



Matee Ullah Khan^a, Misbah Aslam^b, Sohail Anjum Shahzad^{a,*}, Zulfiqar Ali Khan^{c,**}, Nazeer Ahmad Khan^a, Muhammad Ali^{d,***}, Sadia Naz^{a,e}, Jameel Rahman^b, Umar Farooq^a

^a Department of Chemistry, COMSATS University Islamabad, Abbottabad Campus, Abbottabad 22060, Pakistan

^b Department of Chemistry, The Islamia University of Bahawalpur, Bahawalpur 63100, Pakistan

^c Department of Chemistry, Government College University, Faisalabad 38000, Pakistan

^d Natural and Medical Sciences Research Center, University of Nizwa, Nizwa 611, Sultanate of Oman

^e Tianjin Institute of Industrial Biotechnology, Chinese Academy of Sciences, Tianjin 300308, China

ARTICLE INFO

Article history:

Received 1 November 2020

Revised 8 January 2021

Accepted 13 January 2021

Available online 19 January 2021

Keywords:

Synthesis of 1,3-diethyl-2-thiobarbituric acid

Urease inhibition

Structure activity relationship (SAR)

Molecular docking studies

ABSTRACT

A series of thiobarbiturates **4a–4e** and bis-thiobarbiturates analogues **5a–5o** has been synthesized by condensing 1,3-diethylthiobarbituric acid **3** with a variety of aromatic aldehydes with varied structural features and substitution at active methylene position of thiobarbituric acid. Afterward, chemical structures of newly synthesized analogues of thiobarbituric acid were characterized through FT-IR, NMR spectroscopy and mass spectrometry. Subsequently, the inhibitory potential of thiobarbiturates **4a–4e** and bis-thiobarbiturates analogues **5a–5o** against urease enzyme was evaluated. The inhibitory potential of all synthesized analogues in terms of IC_{50} value was observed in the range of 8.42 ± 0.32 to $79.34 \pm 0.52 \mu\text{M}$ by comparing with thiourea (IC_{50} $21.25 \pm 0.15 \mu\text{M}$) as a standard urease inhibitor. Out of these twenty analogues, most of the analogues exhibited potent inhibitory activity against urease. After interesting findings, structure activity relationship (SAR) has been established for all analogues. Docking studies revealed that synthesized analogues interacted with active site residues of bimetallic nickel center of the urease enzyme through, thiolate, π - π stacking and hydrogen bonding interactions.

© 2021 Elsevier B.V. All rights reserved.

1. Introduction

The nickel (Ni) dependent hyperactive urease enzyme (urea amidohydrolase; E.C. 3.5.1.5) belongs to a family of phosphotriesterases and amidohydrolases [1]. It is produced in a different varieties of microorganisms including innumerable bacteria, algae, plants, fungi and invertebrates as well as in soil [2]. Urease enzyme catalyzes the fast conversion of urea into ammonia (NH_3) and carbamic acid, which further disproportionate into carbon dioxide (CO_2) and another molecule of ammonia [3]. Uncontrolled production of ammonia by overexpressed urease is lethal for human cells. The overexpression of urease causes various pathological conditions and damages the cells of living system. It is also

found that various pathological problems trigger the formation of urinary stones. It also involves the progression of other diseases like pyelonephritis, hepatic coma, formation of ammonia, hepatic encephalopathy, urolithiasis as well as urinary catheter encrustation [4]. Urease of *Helicobacter pylori* potentially leads toward the development of various diseases including gastric and peptic ulcers which allows the bacteria to persevere in stomach even at low pH range of stomach during the process of colonization [5,6]. Literature studies reveal that the gastric cancer has been ranked as a fourth most occurring cancer and the second major source of deaths related to cancer in the worldwide [7,8]. In agriculture, the excessive activity of soil urease leads to significant economic and environmental problems through anomalous production of large quantity of ammonia into the surrounding environment during the fertilization process of urea. Subsequently, plants are damaged due to lack of their important nutrients as well as ammonia toxicity and high level of soil pH [9].

Infections caused by over-activity of urease can be treated by inhibiting its activity. Various nitrogen containing heterocycles like bis-thiobarbiturates [10a] are known to exhibit urease inhibitory activity (Fig. 1). These synthetic compounds reduce the enzymatic

* Corresponding author at: Department of Chemistry, COMSATS University Islamabad, Abbottabad Campus, Abbottabad 22060, Pakistan.

** CO-corresponding author at: Department of Chemistry, Government College University Faisalabad, Faisalabad 38000, Pakistan.

*** Co-corresponding author at: Natural and Medical Sciences Research Center, University of Nizwa, Nizwa 611, Sultanate of Oman.

E-mail addresses: sashahzad@cuatd.edu.pk (S.A. Shahzad), zulfiqarchem@gmail.com (Z.A. Khan), m.ali@unizwa.edu.om (M. Ali).

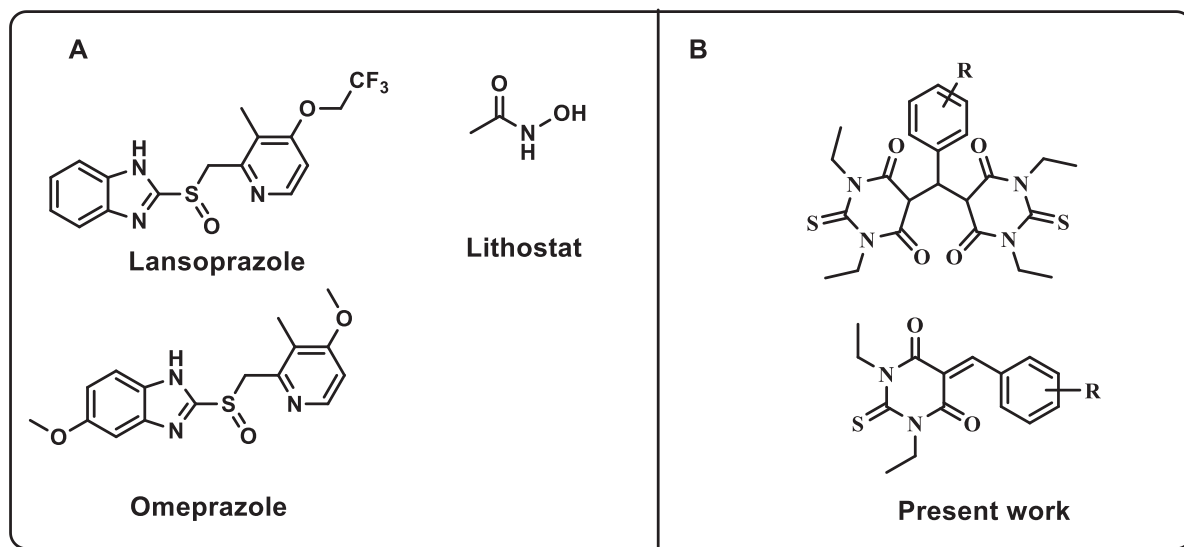


Fig. 1. (A) Clinically used drugs for anti-ulcer (B) Current representative structures of urease inhibitors.

activity of urease by blocking the active site of the enzyme [10]. Such deactivation of urease enzyme leads to reduce its catalytic efficiency for the conversion of urea into ammonia and carbamate or carbon dioxide. A wide variety of urease inhibitors have been examined over the past few years for instance phosphorodiamidates, polyphenols, hydroxamic acid derivatives (Lithostat) and imidazoles like lansoprazole and omeprazole (Fig. 1). However, various side effects including teratogenicity of existing urease inhibitors are reported in literature. Further, *in vivo* usage of many urease inhibitors was prevented owing to their toxicity or structural instability and degradation of phosphoramidates at low pH [11]. Therefore, analogues with high inhibition potential and suitable hydrolytic stability are highly desirable for the possible treatment of urease-based bacterial infections. For this purpose, current research efforts are looking for potent urease inhibitors with high inhibitory activity as well as good hydrolytic stability.

Recently, 1,3-diethylthioarbituric acid and their analogues demonstrated a wide range of pharmacological and biological activities, like use in anesthesia [12], antimicrobial [13], anticonvulsant [14], antifungal [15], antiviral [16], sedative and hypnotics [17], antitumor activities [18], as well as anticancer and anti-inflammatory activities [19,20]. Moreover, thioarbiturate analogues displayed various biological activities like potential mushroom tyrosinase inhibition [21], α -glucosidase inhibition [22], anti-urease [23], antituberculosis [24], anti-proliferative activity [25], radio-sensitization [26], as well as inhibition for diaminopimelate aminotransferase [27]. Discovery of potent urease inhibitors with reduced toxicity and increased structural stability is highly desirable for the treatment of urease mediated infections. Therefore, structurally modified library of 1,3-diethylthioarbituric acid compounds were synthesized and further evaluated for urease inhibition activity.

2. Results and discussion

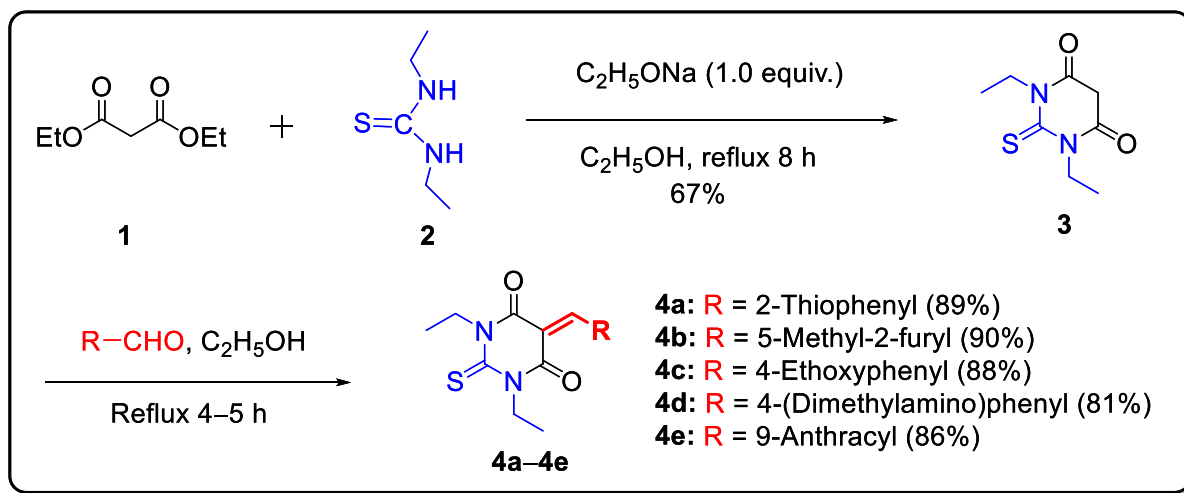
2.1. Chemistry

The recent research for the development of unique urease inhibitors and distinctive biological potential of barbiturates family encouraged us to design new analogues of 1,3-thioarbituric acid for the hope of finding new urease inhibitors with good inhibition potential. A benzimidazole ring in lansoprazole and omepra-

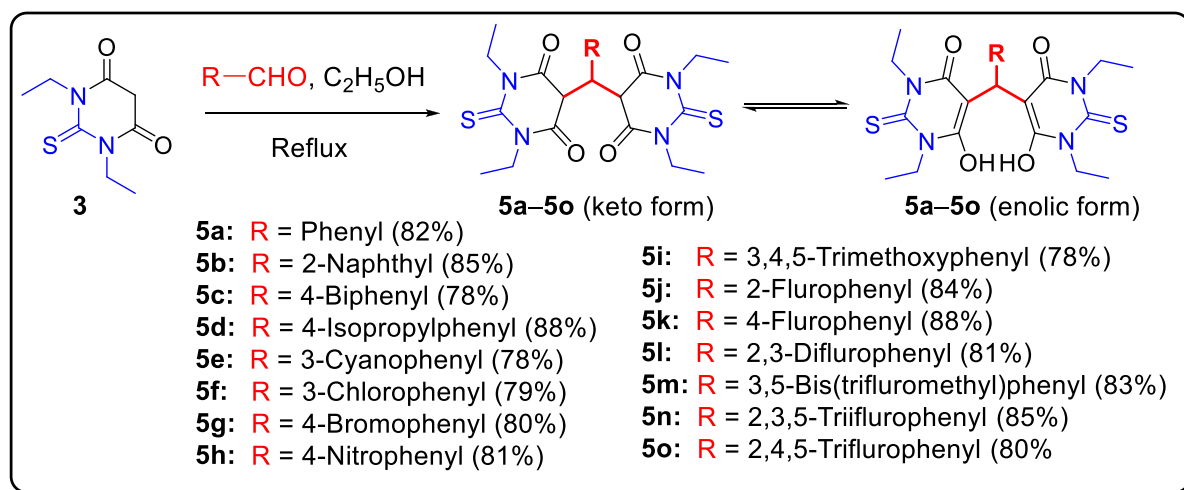
zole has been replaced with a phenyl substituted 1,3-thioarbituric acid moiety to provide more flexibility to accommodate within the urease pocket site [28]. The versatile therapeutic application of 1,3-thioarbituric acid has been advanced by different substitution pattern at aryl ring and functionalization of thioarbituric acid ring system [29]. We believe that nitrogen containing moiety with two carbonyl group and additional presence of thiol group would generate hydrogen bonding site as well as other stabilizing electrostatic interaction within urease pocket [30]. Therefore, a set of thioarbiturates **4a–4e** and bis-thioarbiturates analogues **5a–5o** were synthesized by condensing 1,3-diethylthioarbituric acid **3** with a variety of aromatic aldehydes by using ethanol as a solvent (Scheme 1 & 2). Compounds **4a–4e** were synthesized by treating 1.0 equivalent of 1,3-diethylthioarbituric acid **3** with various aromatic aldehydes (Scheme 1).

However, synthesis of bis-thioarbiturates analogues **5a–5o** was accomplished by treating 2.0 equivalent of 1,3-diethylthioarbituric acid **3** with a range of aromatic aldehydes (Scheme 2). Use of ethanol as a medium of reaction makes this protocol greener and more attractive synthetic method. Electron withdrawing substituted aromatic aldehydes enhance the rate of formation of bis-thioarbiturates analogues with higher yields. Further, additional advantages are associated with a pseudo-three component protocol for preparation of **5a–5o**. These advantages include completion of reaction with reduced time, no need of any base as a catalyst, easy handling of products with high yields and their purification without using column chromatography.

The chemical structures of synthesized analogues of thioarbituric acid were characterized through various spectroscopic methods such as FT-IR, ^1H NMR, ^{13}C NMR and mass spectrometry. In ^1H NMR spectra, appearance of characteristic singlet peak in the range 8.40–8.78 ppm was attributed to CH olefinic moiety and aromatic protons were observed in the range 6.46–9.48 ppm. Presence of these characteristics signals clearly confirm the formation of desired thioarbiturate analogues **4a–4e** (Scheme 1). Similarly, observation of singlet peak attributed to CH bridged proton at 5.60–5.84 ppm and aromatic signals at 6.33–8.19 ppm confirms the formation of bis-thioarbiturates analogues **5a–5o** (Scheme 2). Ring hydrogens in compounds **5a–5o** were not appeared due to presence of keto-enol tautomerism as shown in Scheme 2. Formation of synthesized compounds was further confirmed by mass spectrometry analysis.



Scheme 1. Synthetic protocol for thiobarbituric acid analogues (4a-4e).



Scheme 2. Synthetic protocol for bis-thiobarbituric acid analogues (5a-5o).

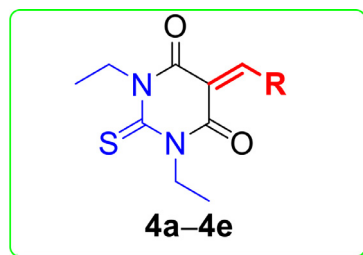
2.2. Urease inhibition studies

Thiobarbituric acid analogues **4a-4e** and bis-thiobarbituric acid analogues **5a-5o** were screened against urease enzyme. All the analogues exhibited various degree of urease inhibition potential with IC₅₀ ranging from 8.42 ± 0.32 to 79.34 ± 0.52 μM by comparing with thiourea (IC₅₀ 21.25 ± 0.15 μM) as a standard urease inhibitor (Tables 1 and 2). The majority of the newly synthesized 1,3-diethylthiobarbituric acid derivatives exhibited potent antiurease activity. The structural core 1,3-diethylthiobarbituric acid remains same in all synthesized compounds as shown in Schemes 1 and 2 and the only changes were made to prepare simple thiobarbituric acid analogues (**4a-4e**) and bis-thiobarbituric acid analogues (**5a-5o**) using different aromatic aldehydes. Structure activity relationship (SAR) revealed urease inhibitory potential mainly based upon various substitutions pattern at phenyl ring (Figs. 2 and 3). The thiophene substituted compound **4a** (IC₅₀ 23.75 ± 0.42), 2-methylfuryl substituted compound **4b** (IC₅₀ 22.53 ± 0.76), 4-ethoxy substituted compound **4c** (IC₅₀ 47.54 ± 0.74), *N,N*-dimethylaminophenyl substituted compound **4d** (IC₅₀ 42.52 ± 0.24) and 9-anthracenyl substituted compound **4e** (IC₅₀ 79.34 ± 0.52 μM) demonstrated promising inhibitory potential (Table 1). Among these analogues, thiophenyl substituted compound **4a** and 2-methylfuryl substituted compound **4b** exhib-

ited potent inhibitory potential (entry 3-4, Table 1). This inhibition potential of both analogues is attributed to lone pair interaction of respective oxygen and sulfur with nickel atom of urease. The smaller difference in inhibitory activity between analogue **4a** and **4b** was observed due to similar electronic and steric nature of thiophenyl and methylfuryl substituted compounds. Introduction of electron-donating groups in the *para* position of phenyl ring for instance 4-ethoxyphenyl substituted compound **4c** and *N,N*-dimethylaminophenyl substituted compound **4d** showed less inhibitory activity (higher IC₅₀ values) as compared to electron withdrawing substituted analogues (Table 1). The urease inhibitory activity decreased in the order of **4b** > **4a** > **4d** > **4c** > **4e**.

Compounds **5a-5c** and **5e-5k** also exhibited potent urease inhibition having IC₅₀ values in the range of 17.31 ± 0.25 to 8.42 ± 0.32 μM that has demonstrated higher inhibitory activity as compared to standard inhibitor thiourea (Table 2). The phenyl analogue **5a** (IC₅₀ 11.56 ± 0.32 μM), naphthyl analogue **5b** (IC₅₀ 12.74 ± 0.21 μM), biphenyl analogue **5c** (IC₅₀ 17.31 ± 0.25 μM), *m*-cyanophenyl analogue **5e** (IC₅₀ 15.11 ± 0.35 μM), 3-chlorophenyl substituted analogue **5f** (IC₅₀ 10.71 ± 0.35 μM), *p*-bromophenyl analogue **5g** (IC₅₀ 11.85 ± 0.32 μM), *p*-nitrophenyl analogue **5h** (IC₅₀ 11.34 ± 0.45 μM), 3,4,5-trimethoxyphenyl analogue **5i** (IC₅₀ 12.32 ± 0.63 μM), *o*-fluorophenyl **5j** (IC₅₀ 8.42 ± 0.32 μM) and

Table 1
Inhibitory activity of urease by thiobarbiturates analogues (4a–4e).

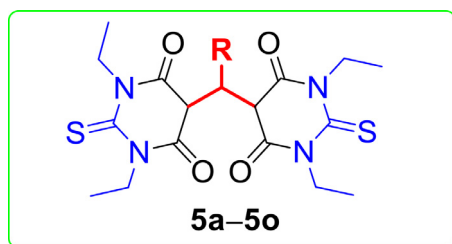


Entry	Compound	R	Yield (%)	IC ₅₀ ± SEM ^a (μM)
1	4a	2-Thiophenyl	89	23.75 ± 0.42
2	4b	5-Methyl-2-furyl	90	22.53 ± 0.76
3	4c	4-Ethoxyphenyl	88	47.54 ± 0.74
4	4d	4-(Dimethylamino)phenyl	81	42.52 ± 0.24
5	4e	9-Anthracyl	86	79.34 ± 0.52
	Thiourea ^b	21.25 ± 0.15		

^a Standard error of the mean ($n = 3$).

^b Standard inhibitor.

Table 2
Inhibitory activity of urease by bis-thiobarbituric acid analogues (5a–5o).



Entry	Compound	R	Yield (%)	IC ₅₀ ± SEM ^a (μM)
1	5a	Phenyl	82	11.56 ± 0.32
2	5b	2-Naphthyl	85	12.74 ± 0.21
3	5c	4-Biphenyl	78	17.31 ± 0.25
4	5d	4-Isopropylphenyl	88	23.24 ± 0.45
5	5e	3-Cyanophenyl	78	15.11 ± 0.35
6	5f	3-Chlorophenyl	79	10.71 ± 0.35
7	5g	4-Bromophenyl	80	11.85 ± 0.32
8	5h	4-Nitrophenyl	81	11.34 ± 0.45
9	5i	3,4,5-Trimethoxyphenyl	78	12.32 ± 0.63
10	5j	2-Fluorophenyl	84	8.42 ± 0.32
11	5k	4-Fluorophenyl	88	9.81 ± 0.32
12	5l	2,3-Difluorophenyl	81	21.43 ± 0.45
13	5m	3,5-Bis-(trifluoromethyl)phenyl	83	25.92 ± 0.34
14	5n	2,3,5-Trifluorophenyl	85	28.54 ± 0.77
15	5o	2,4,5-Trifluorophenyl	80	26.54 ± 0.73
	Thiourea ^b	21.25 ± 0.15		

^a Standard error of the mean ($n = 3$).

^b Standard inhibitor.

p-fluorophenyl analogue **5k** (IC₅₀ 9.81 ± 0.32 μM) showed potent urease inhibition against standard thiourea among twenty synthesized compounds (Table 1–2, Fig. 2 & 3).

At first, it was observed that difference in urease inhibitory activities was found owing to different nature of substituents and their pattern on the phenyl ring. The compound **5a** bearing phenyl group (IC₅₀ 11.56 ± 0.32 μM), compound **5b** having naphthyl group (IC₅₀ 12.74 ± 0.21 μM) and compound **5c** bearing 4-biphenyl group (IC₅₀ 17.31 ± 0.25 μM) demonstrated potent inhibition potential than standard thiourea (Fig. 2). The small difference in inhibitory activity might be due to the presence of similar electronic nature of phenyl, naphthyl and biphenyl groups at the same position (Table 2, Fig. 2). Despite the hydrophobic nature of both biphenyl and 4-isopropylphenyl, the inhibitory activity of biphenyl substituted analogue **5c** is relatively higher than 4-isopropylphenyl sub-

stituted analogue **5d** (IC₅₀ 23.24 ± 0.45 μM) perhaps due to favorable hydrophobic and π - π stacking interactions (Fig. 2).

Analogue **5f** having *m*-chlorophenyl group (IC₅₀ 10.71 ± 0.35 μM) exhibited potent urease inhibition (Fig. 2). This favorable inhibition activity might possibly be due to either hydrogen bonding or any other electrostatic interaction of chloro group with nickel atom of urease. Analogue **5e** bearing *m*-cyanophenyl group (IC₅₀ 15.11 ± 0.35 μM) showed potent inhibitory potential but found less active as compared to **5f** bearing *m*-chlorophenyl group owing to different nature of attached substituent at same position. The *p*-bromo analogue **5g** (IC₅₀ 11.85 ± 0.32 μM) and *p*-nitrophenyl analogue **5h** with IC₅₀ value of 11.34 ± 0.45 μM demonstrated better inhibitory potential as compared to standard thiourea (Table 2). The comparable inhibitory potential of *p*-bromo substituted analogue **5g** as compared to *p*-nitro attached

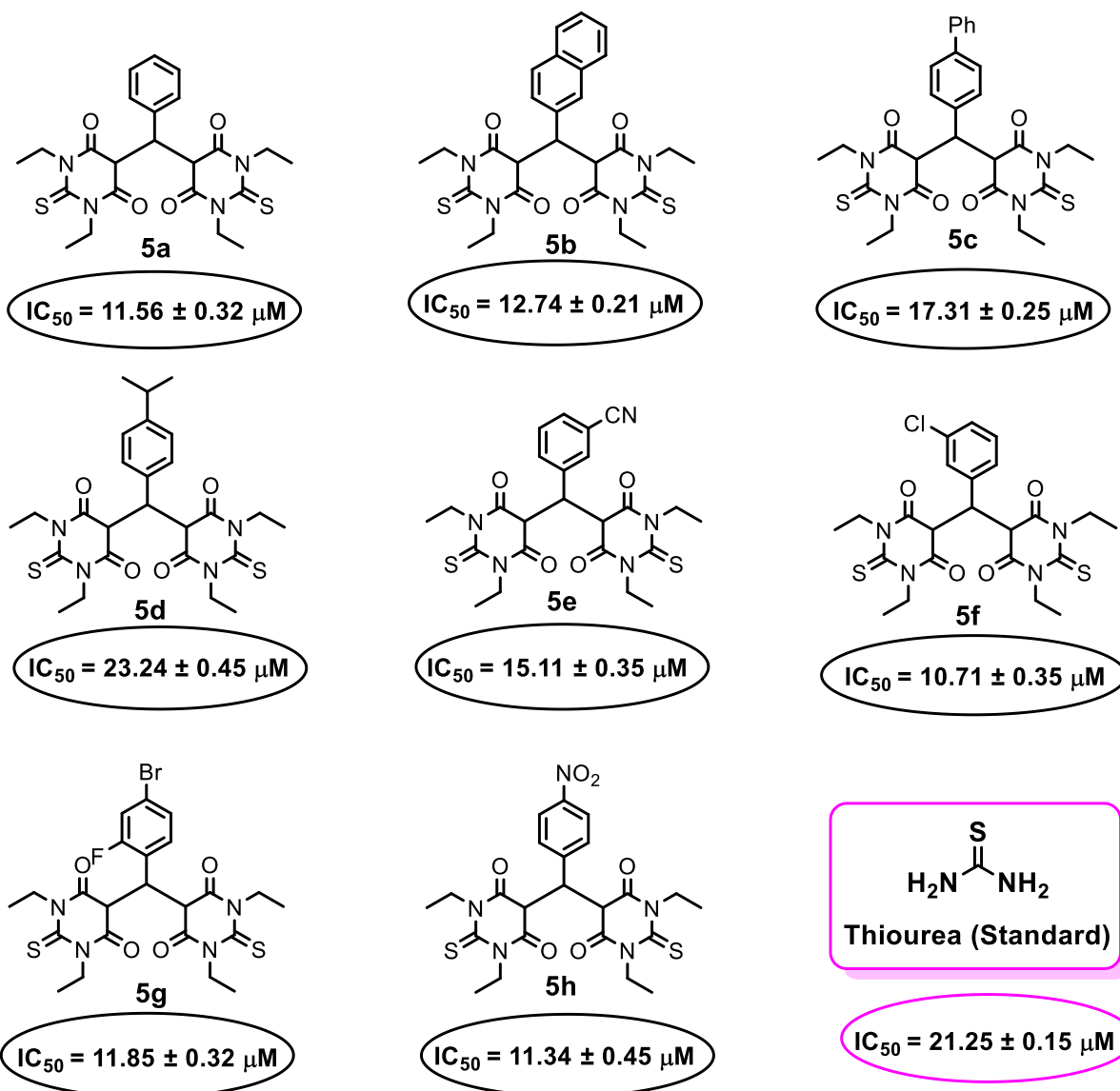


Fig. 2. Nature and position of substituents affect urease inhibitory activity.

Table 3
Binding interactions revealed by molecular docking studies.

S. No.	Compound	Binding interactions
1	4a-series	4a
2		4b
3		4d
4	5-series	5d
5		5f
6		5g
7		5i
8		5j

analogue **5h** might be due to the presence of different nature of electron withdrawing groups at the same position on phenyl ring (Fig. 2). The 3,4,5-trimethoxy analogue **5i** showed potent inhibition potential with IC_{50} value of $12.32 \pm 0.63 \mu\text{M}$ (Table 2). The outstanding inhibition might be due to combined impact of hydrogen bonding of three methoxy groups at benzene ring with

nickel atom in urease enzyme. Despite the electron donating nature of both 4-isopropylphenyl and 3,4,5-trimethoxy groups, the inhibitory activity of 4-isopropylphenyl substituted analogue **5d** ($IC_{50} 23.24 \pm 0.45 \mu\text{M}$) is less than 3,4,5-trimethoxy substituted analogue **5i** (Table 2). It is believed that presence of 4-isopropyl group on phenyl ring ruled out the possibility of hydrogen bonding or $\pi-\pi$ stacking interactions with active site of urease enzyme (Fig. 2). Analogues **5j** and **5k** having *o*-fluoro ($IC_{50} 8.42 \pm 0.32 \mu\text{M}$) and *p*-fluoro ($IC_{50} 9.81 \pm 0.32 \mu\text{M}$) were found the most potent urease inhibitors among synthesized analogues of thiobarbituric acid **4a-4e** and bis-thiobarbituric acid **5a-5o** (Table 2, Fig. 3). It was believed that small difference in inhibitory activity between these two analogues **5j** bearing 2-fluorophenyl and **5k** having 4-fluorophenyl might be due to difference in position of fluoro substituent on the phenyl ring (Fig. 3). Furthermore, presence of fluoro group at phenyl ring may have possibility of either hydrogen bonding or any other favorable electrostatic interaction with nickel atom of urease enzyme. It was also learned that presence of fluoro group at *ortho* position is more effective as compared to *para* position in phenyl ring (Fig. 3). Likewise, 2,3-difluoro substituted analogue **5l** ($IC_{50} 21.43 \pm 0.45 \mu\text{M}$) also

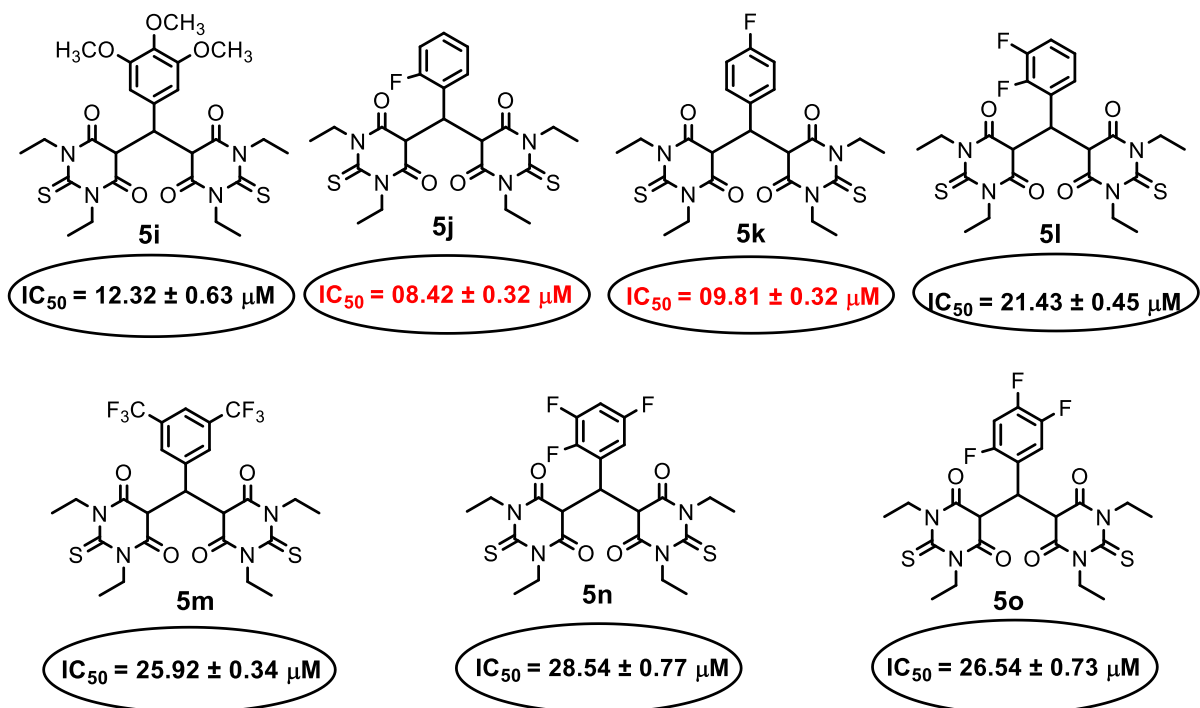


Fig. 3. Relationship of both position and number of fluorine substituents toward urease inhibitory activity.

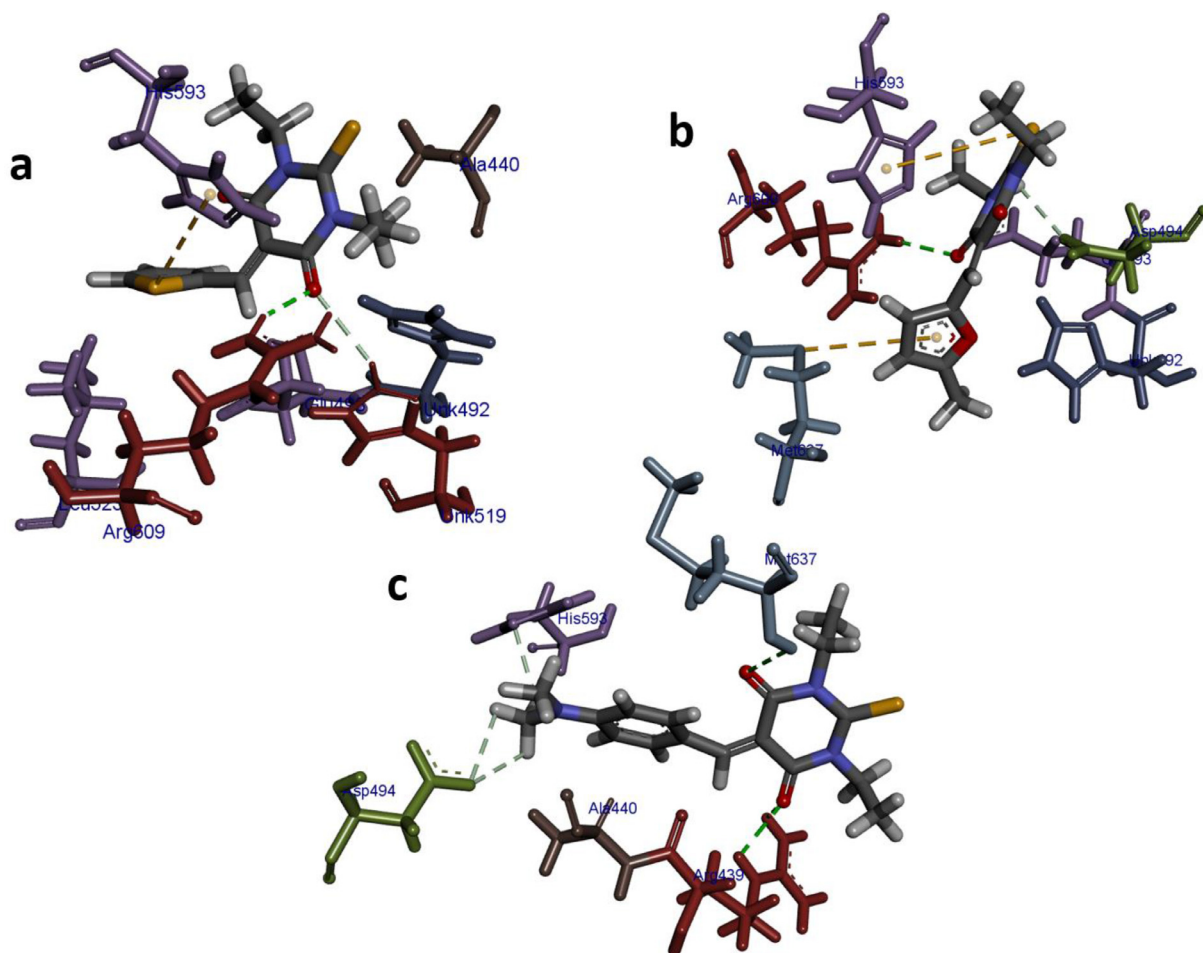


Fig. 4. Binding interactions of most potent inhibitor 4a, 4b and 4d into active pocket of urease (3D-view).

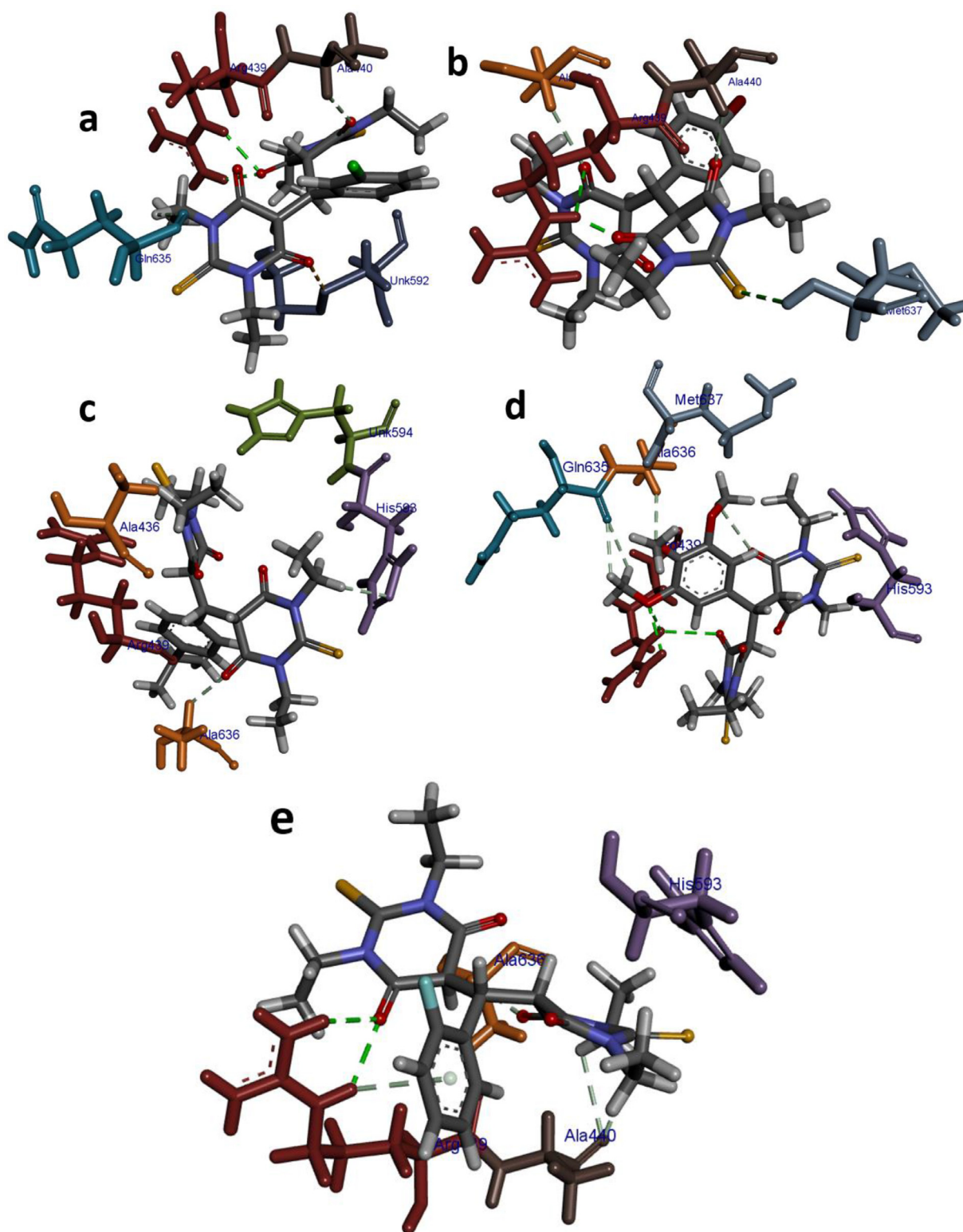


Fig. 5. Binding interaction pattern of compounds (a) 5f, (b) 5g, (c) 5d, (d) 5i and (e) 5j inside active pocket of urease (3D-view).

exhibited potent inhibitory activity (Fig. 3). The inhibitory activity of 2,3-difluoro substituted analogue **5l** might be due to hydrogen bonding or any equivalent binding interaction of highly electronegative two fluoro groups on phenyl ring with nickel atom of urease enzyme. Similarly, 3,5-bis(trifluoromethyl) substituted analogue **5m** (IC_{50} 25.92 ± 0.34 μ M), 2,3,5-trifluorophenyl analogue **5n** (IC_{50} 28.54 ± 0.77 μ M) and 2,4,5-trifluorophenyl ana-

logue **5o** (IC_{50} 26.54 ± 0.73 μ M) also exhibited potent inhibitory potential (Fig. 3). However, strategic impact of number of fluorine groups on phenyl ring was also realized that monofluoro substituted analogues demonstrated better inhibitory activity as compared to presence of di or trifluoro groups on phenyl ring. The inhibitory potential also depends on the position of fluorine group in monofluoro substituted analogues. It is concluded that further

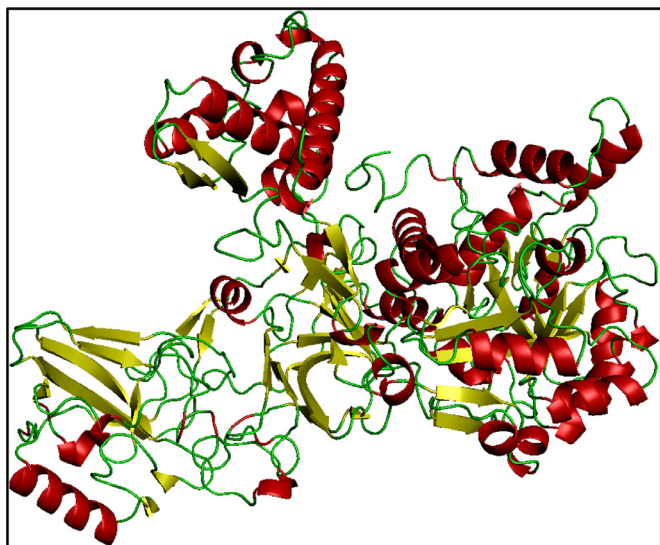


Fig. 6. 3D view of urease from Jack bean (PDB ID: 3LA4).

addition of fluoro groups on phenyl ring will not increase inhibitory activity of urease enzyme.

This SAR clearly demonstrates that electronic and steric nature of substituents are playing important role in urease inhibition. It is also realized that *bis*-thiobarbiturates analogues show more inhibition as compared to thiobarbiturates analogues. The reason might be due more hydrogen bonding site and electrostatic interaction of two pyrimidine rings including unique influence of substitution pattern at phenyl rings. Furthermore, balance between electronic and steric bulk of attached substituents in synthesized analogues of thiobarbituric acid **4a–4e** and *bis*-thiobarbituric acid **5a–5o** is certainly a contributing factor to either increase or decrease their inhibitory potential. For example, anthracyl substituted compound **4e** with IC_{50} value of $79.34 \pm 0.52 \mu M$ exhibited the least inhibitory activity. The reason of this greatly reduced inhibitory activity might be associated to steric bulk of anthracenyl moiety. The SAR showed that the nature and number of substituents as well as substitution pattern greatly affected the inhibitory potential of synthesized compounds. To understand detailed binding interactions of these compounds with urease enzyme, molecular docking was carried out against bimetallic urease enzyme using the MOE software.

2.3. Molecular docking studies

Molecular docking studies of potent inhibitors of both thiobarbiturates analogues (**4a–4e**) alongside *bis*-thiobarbituric acid analogues (**5a–5o**) of urease enzyme were performed for better understanding of their binding interaction pattern into active pocket. The active site of urease has Ni-atoms that could be targeted by competitive inhibitors. The test compounds showed mostly H-bonding interaction, π -sulfur, π -cation and metal contact interaction with active site residues having binding score in the range of -22.05 to -2.73 kcal/mol for **4a–4e** while -21.60 to -4.75 for **5a–5e** series. The best binding scores in case of thiobarbiturates analogues (**4a–4e**) were observed for **4b** (-20.61 kcal/mol), **4a** (-18.95 kcal/mol) and **4d** (-22.05 kcal/mol) involving H-bonding interaction with Arg609 and π -sulfur interaction with His593 in the active pocket as revealed in Fig. 4a–b. Similarly, **4d** also showed good binding interactions with active site residues *i.e.* Met637 (H-bond; 3.08 \AA) and Arg439 (H-bond; 2.44 , 2.54 \AA) having binding score -22.05 kcal/mol as depicted in Fig. 4c and Table 3.

For *bis*-thiobarbituric acid analogues (**5a–5o**) the best binding scores were observed for **5f** (-12.20 kcal/mol), **5g** (-17.49 kcal/mol), **5d** (-17.86 kcal/mol), **5i** (-16.83 kcal/mol) and **5j** (-15.87 kcal/mol). Molecular docking studies revealed that almost all compounds interacted with Arg439 through H-bonding alongside other interactions like π -cation and π -alkyl interactions as depicted in Fig. 5a–5e and Table 3.

3. Conclusion

In summary, twenty analogues of 1,3-diethylthiobarbituric acid were accessed in good yields under convenient reaction conditions. A new diverse range of 1,3-diethylthiobarbituric acid analogues were discovered as potent urease inhibitors. Several newly synthesized analogues of thiobarbiturate and *bis*-thiobarbiturate demonstrated outstanding inhibitory potential (IC_{50} 17.31 ± 0.25 to $8.42 \pm 0.32 \mu M$) as compared to standard thiourea. In addition to excellent inhibitory activity of analogues **5a–5o**, fluorophenyl substituted thiobarbituric acid analogues **5j** and **5k** having *o*-fluoro (IC_{50} $8.42 \pm 0.32 \mu M$) and *p*-fluoro (IC_{50} $9.81 \pm 0.32 \mu M$) showed extraordinary inhibitory activity. The SAR could potentially provide useful insights into the future design of potent urease inhibitors with desired pharmacokinetic properties. Molecular docking studies of *bis*-thiobarbituric acid analogues **5a–5o** presented the best binding scores for **5f** (-12.20 kcal/mol), **5g** (-17.49 kcal/mol), **5d** (-17.86 kcal/mol), **5i** (-16.83 kcal/mol) and **5j** (-15.87 kcal/mol). Molecular docking studies revealed that almost all compounds interacted with Arg439 through H-bonding alongside other interactions like π -cation and π -alkyl interactions. These compounds could be promising leads for further suitable modification to design drug like scaffolds as potent urease inhibitors.

4. Materials and methods

All commercially purchased reagents were used without further purification. The starting reagents were weighed by digital balance and were used at room temperature in the presence of air. 1H NMR and ^{13}C NMR spectra were performed at 300, 400 MHz and 100 MHz respectively using Bruker Avance III HD 400 MHz NMR spectrometer at COMSATS University Islamabad, Abbottabad Campus. $CDCl_3$ was used as deuterated solvent for all NMR analysis. The spectroscopic data was measured in δ (ppm). The NMR peaks were recorded in chemical shifts and corresponding coupling constant were calculated in Hz. Infra-Red spectra (KBr) were performed on a Bruker FT-IR Spectrometer Model Tensor II. The spectra were measured in term of wavenumber (cm^{-1}) of region 4000 – 600 cm^{-1} . The completion of reaction was monitor by thin layer chromatography (TLC) precoated silica gel aluminum plates (Kieselgel 60, F254, Merck, Germany). For the detection of chromatograms, iodine vapors and UV lamp (λ_{max} 254 nm) were used.

4.1. General procedure for the synthesis of 1,3-diethylthiobarbituric acid (3)

In the reaction mixture of diethylmalonate **1** (0.19 g, 1.2 mmol) and 1, 3-diethylthiourea **2** (0.13 g, 1.0 mmol), sodium ethoxide (0.06 g, 1.0 mmol) was added. The above resulting reaction mixture was refluxed for 8 h and white precipitates were appeared. The resulting reaction mixture was diluted with 15 mL hot water and hydrochloric acid was added to make the solution acidic. The clear solution was filtered and cooled for overnight. The resulting white precipitates were filtered. The obtained precipitates were washed with cold water and dried.

4.2. General procedure for the synthesis of thiobarbiturates analogues (4a–4e)

The equivalent amounts of 1,3-diethylthiobarbituric acid **3** (0.20 g, 1.0 mmol) and different aromatic aldehydes (1.0 mmol) were dissolved in ethanol (15 mL). The reaction mixture was refluxed for 4–5 h. The progress of reaction was monitored by thin layer chromatography. After completion of reaction, the precipitates were filtered. The obtained precipitates were washed with cold methanol or cold ethanol (3 × 5 mL) and dried. Finally, recrystallization was completed with mixture of ethanol and chloroform solvents.

4.2.1. 1,3-Diethyl-5-(thiophen-2-ylmethylene)thioxodihydropyrimidine-4,6-dione (4a) [31]

Yellow solid, 89%, M.P 170–172 °C; IR (KBr) ν_{\max} 2980, 1656, 1568, 1394, 1105 cm^{-1} ; ^1H NMR: (CDCl_3 , 300 MHz): δ 8.78 (s, 1H, =CH of olefinic moiety), 8.06 (dd, 1H, $J = 5.1$, 1.2 Hz, ArH), 7.94 (dd, 1H, $J = 4.0$, 1.2 Hz, ArH), 7.33 (dd, 1H, $J = 5.1$, 4.0 Hz, ArH), 4.56–4.65 (m, 4H, 2 × N-CH₂), 1.26–1.38 (m, 6H, 2 × CH₃); ^{13}C NMR (100 MHz, CDCl_3): δ 179.9 (C), 160.9 (C), 159.7 (C), 150.1 (CH), 145.7 (CH), 142.6 (CH), 137.5 (C), 128.5 (CH), 111.4 (C), 44.0 (CH₂), 43.2 (CH₂), 12.4 (CH₃), 12.3 (CH₃); HRMS: m/z calcd for $\text{C}_{13}\text{H}_{14}\text{N}_2\text{O}_2\text{S}_2$ (M^+): 294.0497; found: 294.0519.

4.2.2. 1,3-Diethyl-5-(5-methylfuran-2-yl)methylenethioxodihydropyrimidine-4,6-dione (4b)

Yellow solid, 90%, M.P 159–161 °C; IR (KBr) ν_{\max} 2980, 1662, 1575, 1386, 1104 cm^{-1} ; ^1H NMR: (CDCl_3 , 300 MHz): δ 8.74 (d, 1H, $J = 3.6$ Hz, ArH), 8.40 (s, 1H, =CH of olefinic moiety), 6.46 (d, 1H, $J = 3.9$ Hz, ArH), 4.55–4.63 (m, 4H, 2 × N-CH₂), 2.51 (s, 3H, Ar-CH₃), 1.30–1.36 (m, 6H, 2 × CH₃); ^{13}C NMR (100 MHz, CDCl_3): δ 179.9 (C), 163.9 (C), 161.1 (C), 159.0 (C), 151.0 (C), 141.3 (CH), 131.8 (CH), 113.5 (CH), 110.1 (C), 44.0 (CH₂), 43.3 (CH₂), 14.8 (CH₃), 12.44 (CH₃), 12.40 (CH₃); HRMS: m/z calcd for $\text{C}_{14}\text{H}_{16}\text{N}_2\text{O}_3\text{S}$ (M^+): 292.0882; found: 292.0932.

4.2.3. 5-(4-Ethoxybenzylidene)-1,3-diethylthioxodihydropyrimidine-4,6-dione (4c)

Yellow solid, 88%, M.P 152–154 °C; IR (KBr) ν_{\max} 2983, 1655, 1532, 1379, 1104 cm^{-1} ; ^1H NMR: (CDCl_3 , 400 MHz): δ 8.52 (s, 1H, =CH of olefinic moiety), 8.37 (d, 2H, $J = 8.0$ Hz, ArH), 6.98 (d, 2H, $J = 8.0$ Hz, ArH), 4.56–4.62 (m, 4H, 2 × N-CH₂), 4.17 (q, 2H, $J = 7.0$ Hz, OCH₂), 1.48 (t, 3H, $J = 7.0$ Hz, CH₃ of ethoxy moiety), 1.32–1.36 (m, 6H, 2 × CH₃); ^{13}C NMR (100 MHz, CDCl_3): δ 179.9 (C), 164.3 (C), 161.5 (C), 160.2 (CH), 159.0 (C), 138.4 (2CH), 125.7 (C), 114.8 (C), 114.6 (2CH), 64.1 (CH₂), 44.2 (CH₂), 43.6 (CH₂), 14.6 (CH₃), 12.5 (CH₃), 12.4 (CH₃); HRMS: m/z calcd for $\text{C}_{17}\text{H}_{20}\text{N}_2\text{O}_3\text{S}$ (M^+): 332.1195; found: 332.1232.

4.2.4. 5-(4-dimethylaminobenzylidene)-1,3-diethylthioxodihydropyrimidine-4,6-dione (4d) [32]

Red solid, 81%, M.P 208–210 °C; IR (KBr) ν_{\max} 2983, 1655, 1581, 1342, 1104 cm^{-1} ; ^1H NMR: (CDCl_3 , 400 MHz): δ 8.39–8.45 (m, 3H, ArH & =CH of olefinic moiety), 6.79–6.86 (m, 2H, ArH), 4.57–4.63 (m, 4H, 2 × N-CH₂), 3.19 (s, 6H, 2 × N-CH₃), 1.33–1.36 (m, 6H, 2 × CH₃); ^{13}C NMR (100 MHz, CDCl_3): δ 179.9 (C), 161.2 (C), 160.4 (C), 160.1 (CH), 153.9 (C), 138.4 (2CH), 125.7 (C), 114.8 (C), 110.9 (2CH), 44.18 (CH₂), 43.17 (CH₂), 41.6 (2xCH₃), 12.4 (CH₃), 12.2 (CH₃); HRMS: m/z calcd for $\text{C}_{17}\text{H}_{21}\text{N}_3\text{O}_2\text{S}$ (M^+): 331.1354; found: 331.1384.

4.2.5. 5-(Anthracen-9-ylmethylene)-1,3-diethylthioxodihydropyrimidine-4,6-dione (4e)

Dark blue solid, 86%, M.P 215–217 °C; IR (KBr) ν_{\max} 2927, 1671, 1568, 1394, 1105 cm^{-1} ; ^1H NMR: (CDCl_3 , 400 MHz): δ 9.48 (s, 1H,

ArH), 8.58 (s, 1H, =CH of olefinic moiety), 8.08 (dd, 2H, $J = 6.7$, 1.9 Hz, ArH), 7.88 (dd, 2H, $J = 7.3$, 2.5 Hz, ArH), 7.50–7.55 (m, 4H, ArH), 4.70 (q, 2H, $J = 6.9$ Hz, N-CH₂), 4.34 (q, 2H, $J = 7.0$ Hz, N-CH₂), 1.46 (t, 3H, $J = 7.0$ Hz, CH₃), 1.13 (t, 3H, $J = 7.0$ Hz, CH₃); ^{13}C NMR (100 MHz, CDCl_3): δ 179.0 (C), 159.8 (C), 157.7 (CH), 157.1 (C), 131.0 (2C), 130.2 (2C), 129.3 (2CH), 128.6 (CH), 128.4 (C), 126.9 (2CH), 125.6 (2CH), 125.0 (2CH), 123.4 (C), 44.2 (CH₂), 43.4 (CH₂), 12.6 (CH₃), 12.4 (CH₃); HRMS: m/z calcd for $\text{C}_{23}\text{H}_{20}\text{N}_2\text{O}_2\text{S}$ (M^+): 388.1245; found: 388.1256

4.3. General procedure for the synthesis of bis-thiobarbiturates analogues (5a–5o)

The non-equivalent amounts of 1,3-diethyl-2-thiobarbituric acid **3** (0.40 g, 2.0 mmol) and different aromatic aldehydes (1.0 mmol) were dissolved in ethanol (15 mL). The reaction mixture was refluxed for 3–4 h. The progress of reaction was monitored by thin layer chromatography. After completion of reaction as indicated by TLC, the appeared precipitates were filtered and washed with cold ethanol or cold methanol (3 × 5 mL). Finally, recrystallization was completed with mixture of ethanol and chloroform solvents.

4.3.1. 5,5'-(Phenylmethylene)-bis(1,3-diethylthioxodihydropyrimidine-4,6-dione (5a) [32]

Bright yellow crystals, 82%, M.P 188–190 °C; IR (KBr) ν_{\max} 2978, 1610, 1518, 1378, 1107 cm^{-1} ; ^1H NMR: (CDCl_3 , 400 MHz): δ 7.29–7.36 (m, 3H, ArH), 7.15 (d, 2H, $J = 8.12$ Hz, ArH), 5.69 (s, 1H, -CH-Ar), 4.57–4.73 (m, 8H, 4 × N-CH₂), 1.40 (t, 6H, $J = 7.0$ Hz, 2 × CH₃), 1.31 (t, 6H, $J = 6.9$ Hz, 2 × CH₃); ^{13}C NMR (100 MHz, CDCl_3): δ 174.7 (C), 163.9 (C), 162.4 (C), 135.6 (C), 128.6 (CH), 126.9 (CH), 126.5 (CH), 97.6 (enolized C), 45.3 (2xCH₂), 44.7 (2xCH₂), 35.1 (CH), 12.2 (2xCH₃), 12.1 (2xCH₃); HRMS: m/z calcd for $\text{C}_{23}\text{H}_{28}\text{N}_4\text{O}_4\text{S}_2$ (M^+): 488.1552; found: 488.1563.

4.3.2. 5,5'-(Naphthalen-2-ylmethylene)-bis(1,3-diethylthioxodihydropyrimidine-4,6-dione (5b)

Light yellow powder, 85%, M.P 175–177 °C; IR (KBr) ν_{\max} 2979, 1613, 1505, 1379, 1108 cm^{-1} ; ^1H NMR: (CDCl_3 , 400 MHz): δ 7.80–7.86 (m, 3H, ArH), 7.74–7.77 (m, 1H, ArH), 7.55 (s, 1H, ArH), 7.48–7.50 (m, 2H, ArH), 5.84 (s, 1H, -CH-Ar), 4.59–4.77 (m, 8H, 4 × N-CH₂), 1.43 (t, 6H, $J = 6.9$ Hz, 2 × CH₃), 1.33 (t, 6H, $J = 7.2$ Hz, 2 × CH₃); ^{13}C NMR (100 MHz, CDCl_3): δ 174.7 (C), 164.0 (C), 162.3 (C), 142.2 (CH), 132.6 (C), 132.0 (C), 131.5 (C), 126.6 (CH), 124.9 (CH), 124.5 (CH), 123.8 (CH), 123.6 (CH), 122.2 (CH), 96.7 (enolized C), 45.4 (2xCH₂), 44.8 (2xCH₂), 35.1 (CH), 12.1 (2xCH₃), 12.0 (2xCH₃); HRMS: m/z calcd for $\text{C}_{27}\text{H}_{30}\text{N}_4\text{O}_4\text{S}_2$ (M^+): 538.1708; found: 538.1718.

4.3.3. 5,5'-([1,1'-Biphenyl]-4-ylmethylene)-bis(1,3-diethylthioxodihydropyrimidine-4,6-dione (5c)

Light yellow solid, 78%, M.P 185–187 °C; IR (KBr) ν_{\max} 2968, 1608, 1518, 1378, 1107 cm^{-1} ; ^1H NMR: (CDCl_3 , 400 MHz): δ 7.61–7.63 (m, 2H, ArH), 7.57 (dd, 2H, $J = 6.62$, 1.76 Hz, ArH), 7.43–7.47 (m, 2H, ArH), 7.36–7.38 (m, 1H, ArH), 7.21 (d, 2H, $J = 7.56$ Hz, ArH), 5.71 (s, 1H, -CH-Ar), 4.59–4.75 (m, 8H, 4 × N-CH₂), 1.41 (t, 6H, $J = 7.0$ Hz, 2 × CH₃), 1.33 (t, 6H, $J = 6.9$ Hz, 2 × CH₃); ^{13}C NMR (100 MHz, CDCl_3): δ 174.6 (C), 163.7 (C), 162.3 (C), 140.5 (C), 139.7 (C), 134.6 (C), 128.8 (CH), 127.3 (CH), 127.1 (CH), 127.0 (CH), 126.8 (CH), 97.4 (enolized C), 45.2 (2xCH₂), 44.6 (2xCH₂), 34.8 (CH), 12.1 (2xCH₃), 12.0 (2xCH₃); HRMS: m/z calcd for $\text{C}_{29}\text{H}_{32}\text{N}_4\text{O}_4\text{S}_2$ (M^+): 564.1865; found: 564.1871.

4.3.4. 5,5'-(4-Isopropylphenyl)methylene)-bis(1,3-diethylthioxodihydropyrimidine-4,6-dione (5d)

White powder, 88%, M.P 155–157 °C; IR (KBr) ν_{\max} 2969, 1611, 1514, 1368, 1106 cm^{-1} ; ^1H NMR: (CDCl_3 , 400 MHz): δ 7.18 (d,

2H, $J = 8.2$, ArH), 7.04 (d, 2H, $J = 8.2$, ArH), 5.65 (s, 1H, -CH-Ar), 4.56-4.73 (m, 8H, 4 × N-CH₂), 2.90-2.93 (m, 1H, CH of isopropyl moiety), 1.39 (t, 6H, $J = 7.0$ Hz, 2 × CH₃), 1.32 (t, 6H, $J = 6.9$ Hz, 2 × CH₃), 1.26 (d, $J = 6.9$ Hz, 6H, 2 × CH₃ of isopropyl moiety); ¹³C NMR (100 MHz, CDCl₃): δ 174.7 (C), 163.8 (C), 162.4 (C), 147.5 (C), 132.8 (C), 126.7 (CH), 126.4 (CH), 97.7 (enolized C), 45.3 (2xCH₂), 44.7 (2xCH₂), 34.8 (CH), 33.7 (CH), 24.1 (2xCH₃), 12.23 (2xCH₃), 12.17 (2xCH₃); HRMS: m/z calcd for C₂₆H₃₄N₄O₇S₂ (M⁺): 530.2021; found: 530.2026.

4.3.5. 3-Bis(1,3-diethyl-4,6-dioxothioxohexahydropyrimidin-5-yl)methylbenzotrile (5e)

White solid, 78%, M.P 223–225 °C; IR (KBr) ν_{\max} 2975, 1612, 1507, 1374, 1106 cm⁻¹; ¹H NMR: (CDCl₃, 400 MHz): δ 7.60 (d, 1H, $J = 2.1$ Hz, ArH), 7.39-7.48 (m, 3H, ArH), 5.66 (s, 1H, -CH-Ar), 4.53-4.74 (m, 8H, 4 × N-CH₂), 1.41 (t, 6H, $J = 6.9$ Hz, 2 × CH₃), 1.32 (t, 6H, $J = 6.9$ Hz, 2 × CH₃); ¹³C NMR (100 MHz, CDCl₃): δ 174.7 (C), 164.0 (C), 162.4 (C), 137.7 (C), 131.1 (CH), 130.7 (CH), 130.4 (CH), 129.5 (CH), 118.9 (C), 112.9 (C), 96.6 (enolized C), 45.4 (2xCH₂), 44.8 (2xCH₂), 35.0 (CH), 12.2 (2xCH₃), 12.1 (2xCH₃); HRMS: m/z calcd for C₂₄H₂₇N₅O₄S₂ (M⁺): 513.1504; found: 513.1511.

4.3.6. 5,5'-(3-Chlorophenyl)methylene-bis(1,3-diethylthioxodihydropyrimidine-4,6-dione (5f))

Light yellow solid, 79%, M.P 188–190 °C; IR (KBr) ν_{\max} 2979, 1612, 1507, 1372, 1109 cm⁻¹; ¹H NMR: (CDCl₃, 400 MHz): 7.25-7.27 (m, 2H, ArH), 7.11 (s, 1H, ArH), 7.02-7.05 (m, 1H, ArH), 5.64 (s, 1H, -CH-Ar), 4.49-4.87 (m, 8H, 4 × N-CH₂), 1.38 (t, 6H, $J = 7.0$ Hz, 2 × CH₃), 1.30 (t, 6H, $J = 7.0$ Hz, 2 × CH₃); ¹³C NMR (100 MHz, CDCl₃): δ 174.1 (C), 163.9 (C), 162.1 (C), 136.9 (C), 132.1 (CH), 131.6 (CH), 131.4 (CH), 130.4 (CH), 111.8 (C), 96.7 (enolized C), 45.3 (2xCH₂), 44.3 (2xCH₂), 34.7 (CH), 12.2 (2xCH₃), 11.9 (2xCH₃); HRMS: m/z calcd for C₂₃H₂₇ClN₄O₄S₂ (M⁺): 522.1162; found: 522.1173.

4.3.7. 5,5'-(4-Bromophenyl)methylene-bis(1,3-diethylthioxodihydropyrimidine-4,6-dione (5g) [22])

Light yellow solid, 80%, M.P 185–187 °C; IR (KBr) ν_{\max} 2975, 1610, 1510, 1379, 1107 cm⁻¹; ¹H NMR: (CDCl₃, 400 MHz): δ 7.46 (d, 2H, $J = 8.2$ Hz, ArH), 7.01 (d, 2H, $J = 8.0$ Hz, ArH), 5.60 (s, 1H, -CH-Ar), 4.53-4.66 (m, 8H, 4 × N-CH₂), 1.39 (t, 6H, $J = 6.9$ Hz, 2 × CH₃), 1.31 (t, 6H, $J = 6.9$ Hz, 2 × CH₃); ¹³C NMR (100 MHz, CDCl₃): δ 174.1 (C), 163.7 (C), 162.1 (C), 147.6 (C), 137.3 (C), 133.8 (CH), 128.5 (CH), 123.1 (CH), 121.9 (CH), 96.3 (enolized C), 45.3 (2xCH₂), 44.7 (2xCH₂), 34.9 (CH), 12.3 (2xCH₃), 12.1 (2xCH₃); HRMS: m/z calcd for C₂₃H₂₇BrN₄O₄S₂ (M⁺): 566.0657; found: 566.0662

4.3.8. 5,5'-(4-Nitrophenyl)methylene-bis(1,3-diethylthioxodihydropyrimidine-4,6-dione (5h) [22])

White solid, 81%, M.P 230–232 °C; IR (KBr) ν_{\max} 2979, 1612, 1523, 1376, 1107 cm⁻¹; ¹H NMR: (CDCl₃, 400 MHz): δ 8.15-8.19 (m, 1H, ArH), 8.02 (s, 1H, ArH), 7.50-7.55 (m, 2H, ArH), 5.71 (s, 1H, -CH-Ar), 4.56-4.81 (m, 8H, 4 × N-CH₂), 1.41 (t, 6H, $J = 6.9$ Hz, 2 × CH₃), 1.32 (t, 6H, $J = 6.9$ Hz, 2 × CH₃); ¹³C NMR (100 MHz, CDCl₃): δ 174.8 (C), 164.0 (C), 162.4 (C), 148.7 (C), 138.4 (C), 132.8 (CH), 129.6 (CH), 122.2 (CH), 122.0 (CH), 96.8 (enolized C), 45.4 (2xCH₂), 44.8 (2xCH₂), 35.1 (CH), 12.2 (2xCH₃), 12.1 (2xCH₃); HRMS: m/z calcd for C₂₃H₂₇N₅O₆S₂ (M⁺): 533.1403; found: 533.1410.

4.3.9. 5,5'-(3,4,5-Trimethoxyphenyl)methylene-bis(1,3-diethylthioxodihydropyrimidine-4,6-dione (5i))

Light yellow powder, 78%, M.P 160–162 °C; IR (KBr) ν_{\max} 2978, 1611, 1516, 1375, 1104 cm⁻¹; ¹H NMR: (CDCl₃, 400 MHz): δ 6.33 (d, 2H, $J = 1.04$ Hz, ArH), 5.64 (s, 1H, -CH-Ar), 4.55-4.76 (m, 8H, 4 × N-CH₂), 3.87 (s, 3H, OCH₃), 3.78 (s, 6H, 2xOCH₃), 1.39 (t, 6H,

$J = 7.0$ Hz, 2 × CH₃), 1.33 (t, 6H, $J = 6.9$ Hz, 2 × CH₃); ¹³C NMR (100 MHz, CDCl₃): δ 174.7 (C), 163.8 (C), 162.3 (C), 142.8 (C), 141.8 (C), 126.5 (C), 126.2 (C), 106.9 (CH), 106.3 (CH), 97.5 (enolized C), 53.3 (2xOCH₃), 51.1 (OCH₃), 45.3 (2xCH₂), 44.7 (2xCH₂), 34.5 (CH), 12.2 (2xCH₃), 12.1 (2xCH₃); HRMS: m/z calcd for C₂₆H₃₄N₄O₇S₂ (M⁺): 578.1869; found: 578.1872.

4.3.10. 5,5'-(2-Fluorophenyl)methylene-bis(1,3-diethylthioxodihydropyrimidine-4,6-dione (5j))

White powder, 84%, M.P 175–177 °C; IR (KBr) ν_{\max} 2977, 1609, 1508, 1372, 1102 cm⁻¹; ¹H NMR: (CDCl₃, 400 MHz): δ 7.26-7.31 (m, 1H, ArH), 7.12-7.16 (m, 2H, ArH), 7.00-7.05 (m, 1H, ArH), 5.74 (s, 1H, -CH-Ar), 4.58-4.74 (m, 8H, 4 × N-CH₂), 1.38 (t, 6H, $J = 7.0$ Hz, 2 × CH₃), 1.31 (t, 6H, $J = 7.0$ Hz, 2 × CH₃); ¹³C NMR (100 MHz, CDCl₃): δ 174.6 (C), 163.1 (C), 162.5 (C), 160.0 (d, 1xCH, $J_{C-F} = 204$ Hz), 129.3 (d, 1xCH, $J_{C-F} = 3.0$ Hz), 129.0 (d, 1xCH, $J_{C-F} = 8.0$ Hz), 124.0 (d, 1xCH, $J_{C-F} = 3.0$ Hz), 122.9 (d, 1xCH, $J_{C-F} = 10.0$ Hz), 116.2 (d, 1xCH, $J_{C-F} = 23.0$ Hz), 97.8 (enolized C), 45.3 (2xCH₂), 44.7 (2xCH₂), 31.8 (CH), 12.2 (2xCH₃), 12.1 (2xCH₃); HRMS: m/z calcd for C₂₃H₂₇FN₄O₄S₂ (M⁺): 506.1448; found: 506.1443.

4.3.11. 5,5'-(4-Fluorophenyl)methylene-bis(1,3-diethylthioxodihydropyrimidine-4,6-dione (5k) [22])

White solid, 88%, M.P 192–194 °C; IR (KBr) ν_{\max} 2973, 1615, 1505, 1381, 1109 cm⁻¹; ¹H NMR: (CDCl₃, 400 MHz): δ 7.11-7.13 (m, 2H, ArH), 7.00-7.05 (m, 2H, ArH), 5.64 (s, 1H, -CH-Ar), 4.56-4.72 (m, 8H, 4 × N-CH₂), 1.39 (t, 6H, $J = 7.0$ Hz, 2 × CH₃), 1.31 (t, 6H, $J = 6.9$ Hz, 2 × CH₃); ¹³C NMR (100 MHz, CDCl₃): δ 174.7 (C), 163.9 (C), 162.4 (C), 161.8 (d, 1xCH, $J_{C-F} = 245$ Hz), 131.3 (d, 1xCH, $J_{C-F} = 3.0$ Hz), 128.1 (d, 1xCH, $J_{C-F} = 7.0$ Hz), 115.5 (d, 1xCH, $J_{C-F} = 22$ Hz), 97.5 (enolized C), 45.3 (2xCH₂), 44.7 (2xCH₂), 34.6 (CH), 12.20 (2xCH₃), 12.15 (2xCH₃); HRMS: m/z calcd for C₂₃H₂₇FN₄O₄S₂ (M⁺): 506.1448; found: 506.1652.

4.3.12. 5,5'-((2,3-Difluorophenyl)methylene)-bis(1,3-diethylthioxodihydropyrimidine-4,6-dione (5l))

White powder, 81%, M.P 192–194 °C; IR (KBr) ν_{\max} 2979, 1612, 1507, 1372, 1109 cm⁻¹; ¹H NMR: (CDCl₃, 400 MHz): 7.05-7.13 (m, 2H, ArH), 6.89-6.93 (m, 1H, ArH), 5.76 (s, 1H, -CH-Ar), 4.57-4.71 (m, 8H, 4 × N-CH₂), 1.38 (t, 6H, $J = 7.0$ Hz, 2 × CH₃), 1.31 (t, 6H, $J = 7.0$ Hz, 2 × CH₃); ¹³C NMR (100 MHz, CDCl₃): δ 174.6 (C), 163.1 (C), 162.5 (C), 152.3 (dd, 1C, $J_{C-F} = 254, 14.0$ Hz), 149.1 (dd, 1C, $J_{C-F} = 204, 14.0$ Hz), 125.5 (d, 1C, $J_{C-F} = 7.0$ Hz), 123.9 (br. s, CH), 123.6 (q, 1xCH, $J_{C-F} = 7.0$ Hz), 116.2 (d, 1xCH, $J_{C-F} = 18.0$ Hz), 97.5 (enolized C), 45.3 (2xCH₂), 44.8 (2xCH₂), 31.97 (CH), 12.2 (2xCH₃), 12.1 (2xCH₃); HRMS: m/z calcd for C₂₃H₂₆F₂N₄O₄S₂ (M⁺): 524.1364; found: 524.1391.

4.3.13. 5,5'-(3,5-Bis(trifluoromethyl)phenyl)methylene-bis(1,3-diethylthioxodihydro-pyrimidine-4,6-dione (5m))

White solid, 83%, M.P 205–207 °C; IR (KBr) ν_{\max} 2982, 1614, 1518, 1365, 1110 cm⁻¹; ¹H NMR: (CDCl₃, 400 MHz): δ 7.82 (s, 1H, ArH), 7.57 (s, 2H, ArH), 5.71 (s, 1H, -CH-Ar), 4.62-4.76 (m, 6H, 3 × N-CH₂), 4.47-4.52 (m, 2H, N-CH₂), 1.41 (t, 6H, $J = 7.0$ Hz, 2 × CH₃), 1.30 (t, 6H, $J = 7.0$ Hz, 2 × CH₃); ¹³C NMR (100 MHz, CDCl₃): δ 174.8 (C), 164.1 (C), 162.3 (C), 138.9 (C), 131.8 (q, 1C, $J_{C-F} = 66.0$ Hz), 127.2 (d, 1C, $J_{C-F} = 3.0$ Hz), 124.8 (CH), 122.1 (CH), 120.9 (quintet, 1C), 119.3 (CH), 96.5 (enolized C), 45.4 (2xCH₂), 44.8 (2xCH₂), 35.2 (CH), 12.1 (2xCH₃), 11.9 (2xCH₃); HRMS: m/z calcd for C₂₅H₂₆F₆N₄O₄S₂ (M⁺): 624.1300; found: 624.1205.

4.3.14. 5,5'-(2,3,5-Trifluorophenyl)methylene-bis(1,3-diethylthioxodihydropyrimidine-4,6-dione (5n))

White powder, 85%, M.P 201–203 °C; IR (KBr) ν_{\max} 2979, 1613, 1505, 1372, 1108 cm⁻¹; ¹H NMR: (CDCl₃, 400 MHz): δ 6.88-6.90

(m, 1H, ArH), 6.67-6.69 (m, 1H, ArH), 5.73 (s, 1H, -CH-Ar), 4.57-4.71 (m, 8H, 4 × N-CH₂), 1.38 (t, 6H, J = 7.0 Hz, 2 × CH₃), 1.32 (t, 6H, J = 7.0 Hz, 2 × CH₃); ¹³C NMR (100 MHz, CDCl₃): δ 174.6 (C), 163.2 (C), 162.5 (C), 126.8, 126.7, 111.1, 110.9, 104.5 (dd, J_{C-F} = 22.0, 21.0 Hz, CH), 104.5 (CH), 97.0 (enolized C), 45.3 (2xCH₂), 44.8 (2xCH₂), 32.1 (CH), 12.1 (2xCH₃), 12.0 (2xCH₃); HRMS: m/z calcd for C₂₃H₂₅F₃N₄O₄S₂ (M⁺): 542.1269; found: 542.1275.

4.3.15. 5,5'-(2,4,5-Trifluorophenyl)methylene-bis(1,3-diethylthioxodihydropyrimidine-4,6-dione (5o)

White solid, 80%, M.P 180–182 °C; IR (KBr) ν_{max} 2977, 1610, 1513, 1379, 1108 cm⁻¹; ¹H NMR: (CDCl₃, 400 MHz): δ 6.87-7.02 (m, 2H, ArH), 5.67 (s, 1H, -CH-Ar), 4.57-4.69 (m, 8H, 4 × N-CH₂), 1.38 (t, 6H, J = 7.0 Hz, 2 × CH₃), 1.32 (t, 6H, J = 7.0 Hz, 2 × CH₃); ¹³C NMR (100 MHz, CDCl₃): δ 174.1 (C), 163.7 (C), 162.1 (C), 136.7 (C), 121.1 (C), 120.8 (C), 107.7 (C), 106.5 (CH), 103.1 (CH), 96.6 (enolized C), 45.4 (2xCH₂), 44.9 (2xCH₂), 32.4 (CH), 12.7 (2xCH₃), 11.9 (2xCH₃); HRMS: m/z calcd for C₂₃H₂₅F₃N₄O₄S₂ (M⁺): 542.1269; found: 542.1276.

4.4. Urease inhibition assay

The previously described Berthelot assay with slight modifications was carried out to evaluate urease inhibitory activity [33,34]. A total volume of 85 μL assay mixture contained 25 μL of 50 mM phosphate buffer, pH 7, 10 μL of test compound, and 10 μL of urease enzyme solution (0.015 units, jack bean urease from Sigma). The contents were preincubated at 37 °C for 10 min. Then, 40 μL of 20 mM substrate (urea) was added per well and re-incubated for further 10 min. After this, contents were pre-read at 625 nm using 96-well plate reader Synergy HT (BioTek Inc. USA). Then freshly prepared mixture of phenol (45 μL) and alkali reagent (70 μL) was added per well. For color development, incubation was continued for further 10 min and then absorbance was noted at 625 nm. The percentage inhibition was calculated by using this formula.

$$\text{Inhibition (\%)} = 100 - [(\text{Abs. of sample} / \text{Abs. of control}) \times 100]$$

Serial dilutions of active compounds were assayed, and their percent inhibitions were determined, and data obtained was used to calculate IC₅₀ values using EZ-Fit Enzyme software (Perrella Inc., USA).

4.5. Molecular docking studies

The compounds of both series, (a) thiobarbiturates analogues (**4a–4e**) and (b) bis-thiobarbituric acid analogues (**5a–5o**) showing highest inhibition potential against urease enzyme were subjected to molecular docking studies to evaluate their binding into the active pocket of urease (Fig. 6). The 3D-structure of urease from Jack bean was retrieved from Protein data bank (PDB ID: 3LA4, Resolution: 2.05 Å) [35]. Molecular operating environment (MOE) software was employed for docking studies [36].

Protein structure preparation was done by removing water molecules, addition of hydrogen atoms, and energy optimization using default force field. Builder program of MOE was employed to acquire modeled chemical structures of synthesized compounds. The default parameters of MOE energy minimization algorithm [gradient: 0.05, Force Field: MMFF94X] were employed to carry out the 3D protonation and energy minimization of the protein. The active site of the enzyme was demarcated within 10 Å of the co-crystallized ligand. The ligand-enzyme interactions in 2D format were calculated using ligand-interaction module of MOE. The MOE and discovery studio visualizer were employed to view docking results and analysis of their surface with graphical representations.

Declaration of Competing Interest

The authors declare that they have no known competing financial interests or personal relationships that could have appeared to influence the work reported in this paper.

CRediT authorship contribution statement

Matee Ullah Khan: Conceptualization, Methodology, Writing - original draft. **Misbah Aslam:** Investigation, Methodology, Visualization. **Sohail Anjum Shahzad:** Funding acquisition, Investigation, Project administration, Supervision, Writing - review & editing. **Zulfiqar Ali Khan:** Data curation, Visualization, Writing - review & editing. **Nazeer Ahmad Khan:** Investigation, Visualization. **Muhammad Ali:** Funding acquisition, Project administration, Supervision, Visualization. **Sadia Naz:** Formal analysis, Software, Validation. **Jameel Rahman:** Investigation, Methodology, Validation, Visualization.

Acknowledgments

The authors are grateful to HEC Pakistan for providing a research grant vide 20-1933/NRPU/R&D/HEC/12/5017. Dr. S. A. Shahzad would like to acknowledge HEC Pakistan for financial support under Project No. 5290/Federal/NRPU/R&D/HEC/2016.

Supplementary materials

Supplementary material associated with this article can be found, in the online version, at doi:10.1016/j.molstruc.2021.129959.

References

- [1] L. Holm, C. Sander, An evolutionary treasure: unification of a broad set of amidohydrolases related to urease, *Proteins: Struct. Funct. Bioinf.* 28 (1997) 72–82.
- [2] C. Follmer, Insights into the role and structure of plant ureases, *Phytochemistry* 69 (1) (2008) 18–28.
- [3] M.J. Maroney, S. Ciurli, Nonredox nickel enzymes, *Chem. Rev.* 114 (2014) 4206–4228.
- [4] H. Mobley, R. Hausinger, Microbial ureases: significance, regulation, and molecular characterization, *Microbiol. Mol. Biol. Rev.* 53 (1989) 85–108.
- [5] H. Mobley, M.D. Island, R.P. Hausinger, Molecular biology of microbial ureases, *Microbiol. Mol. Biol. Rev.* 59 (3) (1995) 451–480.
- [6] C. Montecucco, R. Rappuoli, Living dangerously: how *Helicobacter pylori* survives in the human stomach, *Nat. Rev. Mol. Cell Biol.* 2 (2001) 457–466.
- [7] C.P. Howson, T. Hiyama, E.L. Wynder, The decline in gastric cancer: epidemiology of an unplanned triumph, *Epidemiol. Rev.* 8 (1986) 1–27.
- [8] D.M. Parkin, E.I. Bray, S. Devesa, Cancer burden in the year 2000. The global picture, *Eur. J. Cancer* 37 (2001) 4–66.
- [9] J. Bremner, in: Recent Research on Problems in the Use of Urea as a Nitrogen Fertilizer, *Nitrogen Economy in Tropical Soils*, Springer, 1995, pp. 321–329.
- [10] (a) D. Insuasty, J. Castillo, D. Becerra, H. Rojas, R. Abonia, Synthesis of biologically active molecules through multicomponent reactions, *Molecules* 25 (2020) 505; (b) B. Krajewska, W. Zaborska, Jack bean urease: the effect of active-site binding inhibitors on the reactivity of enzyme thiol groups, *Bioorg. Chem.* 35 (2007) 355–365; (c) M.T. Shehzad, A. Khan, M. Islam, A. Hameed, M. Khat, S.A. Halim, M.U. Anwar, S.R. Shah, J. Hussain, R. Csuk, S. Khan, A. Al-Harrasi, Z. Shafiq, Synthesis and urease inhibitory activity of 1,4-benzodioxane-based thiosemicarbazones: biochemical and computational approach, *J. Mol. Struct.* 1209 (2020) 127922.
- [11] Z. Amtul, R. Siddiqui, M. Choudhary, Chemistry and mechanism of urease inhibition, *Curr. Med. Chem.* 9 (2002) 1323–1348.
- [12] P.A. Steen, J.D. Michenfelder, Cerebral protection with barbiturates: relation to anesthetic effect, *Stroke* 9 (2) (1978) 140–142.
- [13] V.V. Dabholkar, D.T. Ravi, Synthesis of Biginelli products of thiobarbituric acids and their antimicrobial activity, *J. Serb. Chem. Soc.* 75 (2010) 1033–1040.
- [14] V. Srivastava, A. Kumar, Synthesis of some newer derivatives of substituted quinazolinonyl-2-oxo/thiobarbituric acid as potent anticonvulsant agents, *Bioorg. Med. Chem.* 12 (2004) 1257–1264.
- [15] M. Kidwai, R. Thakur, R. Mohan, Ecofriendly synthesis of novel antifungal (thio)barbituric acid derivatives, *Acta Chim. Slov.* 52 (2005) 88–92.
- [16] V. Balas, I. Verginadis, G. Geromichalos, N. Kourkoumelis, L. Male, M. Hursthouse, K. Repana, E. Yiannaki, K. Charalabopoulos, T. Bakas, Synthesis, structural characterization and biological studies of the triphenyltin (IV) complex with 2-thiobarbituric acid, *Eur. J. Med. Chem.* 46 (7) (2011) 2835–2844.
- [17] W.W. Morgan, Abuse liability of barbiturates and other sedative-hypnotics, *Adv. Alcohol Subst. Abuse* 9 (1990) 67–82.

- [18] A.D. Brewer, J.A. Minatelli, J. Plowman, K.D. Paull, V. Narayanan, 5-(N-phenylcarboxamido)-2-thiobarbituric acid (NSC 336628), a novel potential antitumor agent, *Biochem. Pharmacol.* 34 (11) (1985) 2047–2050.
- [19] N.R. Penthala, P.R. Ponugoti, V. Kasam, P.A. Crooks, 5-((1-Aroyl-1*H*-indol-3-yl)methylene)-2-thioxodihydropyrimidine-4,6 (1*H*,5*H*)-diones as potential anti-cancer agents with anti-inflammatory properties, *Bioorg. Med. Chem. Lett.* 23 (5) (2013) 1442–1446.
- [20] A. Barakat, M.S. Islam, A.M. Al-Majid, H.A. Ghabbour, S. Yousuf, M. Ashraf, N.N. Shaikh, M.I. Choudhary, R. Khalil, Z. Ul-Haq, Synthesis of pyrimidine-2,4,6-trione derivatives: anti-oxidant, anti-cancer, α -glucosidase, β -glucuronidase inhibition and their molecular docking studies, *Bioorg. Chem.* 68 (2016) 72–79.
- [21] Q. Yan, R. Cao, W. Yi, L. Yu, Z. Chen, L. Ma, H. Song, Synthesis and evaluation of 5-benzylidene (thio) barbiturate- β -D-glycosides as mushroom tyrosinase inhibitors, *Bioorg. Med. Chem. Lett.* 19 (2009) 4055–4058.
- [22] A. Barakat, M. Ali, A.M. Al-Majid, S. Yousuf, M.I. Choudhary, R. Khalil, Z. Ul-Haq, Synthesis of thiobarbituric acid derivatives: *in vitro* α -glucosidase inhibition and molecular docking studies, *Bioorg. Chem.* 75 (2017) 99–105.
- [23] M. Biglar, R. Mirzazadeh, M. Asadi, S. Sepehri, Y. Valizadeh, Y. Sarrafi, M. Amanlou, B. Larjani, M. Mohammadi-Khanaposhtani, M. Mahdavi, Novel *N,N*-dimethylbarbituric-pyridinium derivatives as potent urease inhibitors: synthesis, *in vitro* and *in silico* studies, *Bioorg. Chem.* 95 (2020) 103529.
- [24] S.V. Laxmi, Y.T. Reddy, B.S. Kuarm, P.N. Reddy, P.A. Crooks, B. Rajitha, Synthesis and evaluation of chromenyl barbiturates and thiobarbiturates as potential antitubercular agents, *Bioorg. Med. Chem. Lett.* 21 (2011) 4329–4331.
- [25] N.R. Madadi, N.R. Penthala, V. Janganani, P.A. Crooks, Synthesis and anti-proliferative activity of aromatic substituted 5-((1-benzyl-1*H*-indol-3-yl)methylene)-1,3-dimethylpyrimidine-2,4,6 (1*H*,3*H*,5*H*)-trione analogs against human tumor cell lines, *Bioorg. Med. Chem. Lett.* 24 (2014) 601–603.
- [26] Y.T. Reddy, K.R. Sekhar, N. Sasi, P.N. Reddy, M.L. Freeman, P.A. Crooks, Novel substituted (Z)-5-((N-benzyl-1*H*-indol-3-yl)methylene) imidazolidine-2,4-diones and 5-((N-benzyl-1*H*-indol-3-yl)methylene) pyrimidine-2,4,6 (1*H*,3*H*,5*H*)-triones as potent radio-sensitizing agents, *Bioorg. Med. Chem. Lett.* 20 (2010) 600–602.
- [27] C. Fan, M.D. Clay, M.K. Deyholos, J.C. Vederas, Exploration of inhibitors for diaminopimelate aminotransferase, *Biorg. Med. Chem.* 18 (2010) 2141–2151.
- [28] Y. Zeng, Y. Ye, D. Liang, C. Guo, L. Li, Meta-analysis of the efficacy of lansoprazole and omeprazole for the treatment of *H. pylori*-associated duodenal ulcer, *Int. J. Physiol. Pathophysiol. Pharmacol.* 7 (2015) 158.
- [29] A. Ashnagar, N. Gharib Naseri, B. Sheeri, Novel synthesis of barbiturates, *Chin. J. Chem.* 25 (2007) 382–384.
- [30] B. Krajewska, Ureasas I. Functional, catalytic and kinetic properties: a review, *J. Mol. Catal. B. Enzym.* 59 (2009) 9–21.
- [31] K.M. Khan, F. Rahim, A. Khan, M. Shabeer, S. Hussain, W. Rehman, M. Taha, M. Khan, S. Perveen, M.I. Choudhary, Synthesis and structure–activity relationship of thiobarbituric acid derivatives as potent inhibitors of urease, *Bioorg. Med. Chem.* 22 (2014) 4119–4123.
- [32] B. Coe, H. Grassam, J. Jeffery, S. Coles, M. Hursthouse, Reactions of 1,3-diethyl-2-thiobarbituric acid with aldehydes: formation of arylbis (1,3-diethyl-2-thiobarbitur-5-yl) methanes and crystallographic evidence for ground state polarisation in 1,3-diethyl-5-[4-(dimethylamino)benzylidene]-2-thiobarbituric acid, *J. Chem. Soc. Perkin Trans. 1* (1999) 2483–2488.
- [33] M. Weatherburn, Phenol-hypochlorite reaction for determination of ammonia, *Anal. Chem.* 39 (1967) 971–974.
- [34] F. Rahim, K. Zaman, H. Ullah, M. Taha, A. Wadood, M.T. Javed, W. Rehman, M. Ashraf, R. Uddin, I. Uddin, Synthesis of 4-thiazolidinone analogs as potent *in vitro* anti-urease agents, *Bioorg. Chem.* 63 (2015) 123–131.
- [35] A. Balasubramanian, K. Ponnuraj, Crystal structure of the first plant urease from jack bean: 83 Years of journey from its first crystal to molecular structure, *J. Mol. Biol.* 400 (2010) 274–283.
- [36] S. Vilar, G. Cozza, S. Moro, Medicinal chemistry and the molecular operating environment (MOE): application of QSAR and molecular docking to drug discovery, *Curr. Top. Med. Chem.* 8 (2008) 1555–1572.